ARTICLE

Robust and biocompatible catalysts for efficient hydrogen-driven microbial electrosynthesis

Frauke Kracke [1], Andrew Barnabas Wong [2], Karen Maegaard [3], Joerg S. Deutzmann [1],
McKenzie A. Hubert [2], Christopher Hahn[2,4], Thomas F. Jaramillo [2,4] & Alfred M. Spormann[1,2]

CO_2 reduction by combined electro- and bio-catalytic reactions is a promising technology platform for sustainable production of chemicals from CO_2 and electricity. While heterogeneous electrocatalysts can reduce CO_2 to a variety of organic compounds at relatively high reaction rates, these catalysts have limitations achieving high selectivity for any single product beyond CO. Conversely, microbial CO_2 reduction pathways proceed at high selectivity; however, the rates at bio-cathodes using direct electron supply via electricity are commonly limiting. Here we demonstrate the use of non-precious metal cathodes that produce hydrogen *in situ* to support microbial CO_2 reduction to C_1 and C_2 compounds. CoP, MoS_2 and NiMo cathodes perform durable hydrogen evolution under biologically relevant conditions, and the integrated system achieves coulombic efficiencies close to 100% without accumulating hydrogen. Moreover, the one-reactor hybrid platform is successfully used for efficient acetate production from electricity and CO_2 by microbes previously reported to be inactive in bioelectrochemical systems.

[1] Department of Civil & Environmental Engineering, Stanford University, Stanford 94305 CA, USA. [2] Department of Chemical Engineering, Stanford University, Stanford 94305 CA, USA. [3] Department of Bioscience, Section for Microbiology, Aarhus University, Aarhus 8000, Denmark. [4] SUNCAT Center for Interface Science and Catalysis, SLAC National Accelerator Laboratory, Menlo Park 94025 CA, USA. Correspondence and requests for materials should be addressed to A.M.S. (email: spormann@stanford.edu)

C O_2 as a sole carbon source offers an attractive platform for the sustainable production of chemicals and fuels, with the potential to avoid emitting annually 38.2 billion tons of this greenhouse gas while increasing the independence from fossil resources. Renewable energy technologies are providing new and competitive alternatives for production processes based on (bio) electrochemical reduction of CO_2 to chemicals[1,2]. Assuming that these chemicals can be combusted as fuels, a carbon-neutral fuel and chemical cycle can be envisioned (cf. Fig. 1a).

A significant advantage of heterogeneous electrocatalysis processes for reducing CO_2 to C_1 and C_{2+} compounds are high reaction rates in relatively mild reaction conditions[3–6]. However, selectivity to multi-carbon compounds remains a major challenge, leading to low energy efficiencies and mixed product streams[3,6–8]. In addition, insufficient long-term stability of the electrocatalytic performance presents a key issue that must be overcome for practical implementation[3,9–14]. Microbial CO_2 reduction reactions, on the other hand, are highly specific, selective, and stable. Moreover, metabolic engineering approaches continuously broaden the product spectrum to include high-value chemicals of industrial relevance[15,16]. Natural electron donors for microbial CO_2 reduction processes are H_2 and CO and direct supply of electrons for microbial metabolism via a cathode has been demonstrated in microbial electrosynthesis[17,18]. Several industrially relevant chemicals such as methane, acetic acid, butyric acid, isobutyric acid, hexanoic acid, ethanol, isopropanol, butanol, isobutanol, and hexanol have been shown to be produced via microbial electrosynthesis from CO_2 and electricity[19–23]. However, these processes currently remain limited by low direct electron uptake rates from the cathode and by a limited number of microbes that are able to directly acquire electrons from solid state electrodes for CO_2 reduction[18,24]. Thus, an integrated platform that combines the advantages of rapid electrochemical reduction reactions with highly selective microbial syntheses is desirable.

The common electron donor for microbial CO_2 reduction is molecular hydrogen, which can be produced electrochemically via the well-established hydrogen evolution reaction (HER). HER is kinetically more facile than electrochemical CO_2 reduction and achieves simultaneously high current densities and selectivity[25]. Hybrid processes have been proposed that couple the electrocatalytic H_2 production in one process to microbial CO_2 reduction in a second microbial gas fermentation step for the production of chemicals[26–28]. However, such two-step processes entail the pumping and mixing of a low-soluble and explosive gas (H_2) at significant costs and safety risks[29].

In fact, most bioelectrochemical CO_2 reduction platforms seem to be driven by molecular hydrogen as intermediate[30]. The cathode material of choice in these systems is commonly carbon-based due to its low price and proven biocompatibility. However, production rates in microbial electrosynthesis can be increased significantly by modifying the cathode material towards more efficient HER, e.g., by introducing transition metals, such as nickel[31,32]. And while a direct integration of electro- and microbial-catalysis with H_2 as an intermediate offers the possibility to increase overall electron transfer rates, it also presents a significant challenge, because the optimal environmental conditions for both processes differ substantially. While the electrocatalytic HER is best controlled under either strong acidic or alkaline conditions and in ultra-pure electrolytes, microbial synthesis proceeds at circumneutral pH, in the presence of essential media supplements (e.g. trace metals and vitamins) and with high concentrations of CO_2. Severe deactivation of inorganic catalysts by microbial growth media components was observed in previous studies[33] as well as toxic effects towards the microorganisms caused by dissolution of the cathode material[34].

Due to their high electrochemical stability, transition-metal-based electrode materials were identified as particularly promising, and sustainable alternatives to Pt as catalysts for HER[35–37]. Here, we select the inexpensive, earth-abundant cobalt-phosphide (CoP), molybdenum-disulfide (MoS_2), and nickel–molybdenum alloy (NiMo) as cathode materials as these show particularly promising properties at circumneutral pH[35,36,38]. We test their biocompatibility in a directly integrated bioelectrochemical system for production of chemicals from electricity and CO_2 (cf. Fig. 1b), and characterize the electrochemical stability of the different materials under biologically relevant conditions. Using methanogenic archaea and homoacetogenic bacteria, we
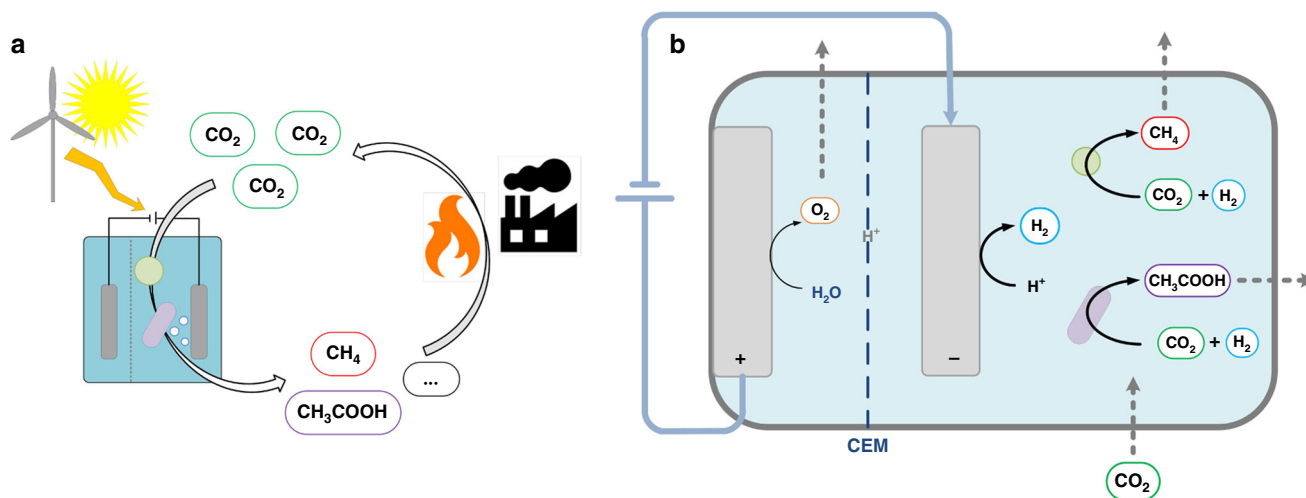

Fig. 1 Process overview. Schematic of a directly integrated bioelectrochemical system for sustainable production of chemicals from electricity and inorganic carbon. **a** Illustration of the envisioned carbon-neutral economy. **b** Integrated bioelectrochemical reactor; anode (+) and cathode (−) compartments are separated by a proton-exchange membrane (CEM). The target reaction on the cathode is the evolution of hydrogen as an electron donor for the microbial reduction of CO_2. The displayed microbial catalysts are homoacetogenic bacteria (purple rod) and methanogenic archaea (green cocci) as demonstrated in the presented study. Efficient conversion of electricity and CO_2 is achieved for the target products acetate and methane, respectively, via highly biocompatible transition-metal-based cathodes in microbial growth media (Coulombic efficiency near 100%). The system can be powered by any electricity source including renewable sources

demonstrate stable and high rates of CO_2 reduction to methane and acetate, respectively, at coulombic efficiencies of close to 100% and thereby a successfully integrated platform.

Results

Biocompatible hydrogen production by non-precious metal cathodes. We first characterized hydrogen production rates of cathodes with CoP, MoS_2, and NiMo as HER catalysts in pure bicarbonate buffer as an approximation for a biocompatible electrolyte for microbial CO_2 reduction at neutral pH. Platinum was used as the reference catalyst for the HER in all experiments. The catalysts were prepared on planar silicon substrates of identical geometric surface areas. The resulting flat electrode surface enables direct comparison of the biocompatibility of the different materials in the integrated conditions by minimizing any convoluting effects introduced by surface roughness of the catalysts. The here presented rates were integrated over a period of 3 h to emphasize the long-term rather than initial performance.

At neutral pH in CO_2-sparged aqueous solutions (0.03 M $NaHCO_3$, pH 7), all three catalysts produced hydrogen at rates in the same order of magnitude as the benchmark catalyst platinum (see Fig. 2a and Supplementary Table 1). At all tested potentials (−0.6 to −1 V vs standard hydrogen electrode (SHE)) NiMo electrodes outperformed Pt, while the performances of the CoP and MoS_2 electrodes was constantly lower than that of Pt. This trend became more pronounced with decreasing cathode potential. The highest H_2 production rate of 48.0 ± 1.5 μmol h^{-1} cm^{-2} was observed for the NiMo alloy at a potential of −1 V vs SHE and a coulombic efficiency of $98.0 \pm 3.1\%$. At the same working electrode potential, platinum achieved an average H_2 production rate of 39.0 ± 1.5 μmol h^{-1} cm^{-2} at a CE of $99.0 \pm 3.8\%$. The H_2 production on CoP and MoS_2 cathodes occurred at average rates of 11.1 ± 1.6 μmol h^{-1} cm^{-2} and 10.0 ± 1.1 μmol h^{-1} cm^{-2} and CEs of $94.1 \pm 13.6\%$ and $94.0 \pm 9.2\%$, respectively. It is noteworthy that the HER performance can be significantly impacted by electrochemical conditions such as pH[39,40], CO_2 exposure[40–42], and buffering anion concentration[43,44]. While a direct comparison to other state-of-the-art catalysts is challenging due to the aforementioned factors, the results clearly indicate that all tested catalysts can achieve favorable hydrogen production rates for biointegration, with the NiMo alloy presenting the most promising material under the conditions tested.

Next, the activities of the different electrodes were characterized in the presence of different microbial growth media to evaluate their sensitivity towards required microbial media additions to the electrolyte. When tested in the presence of a yeast extract-containing complex medium used for growth of homoacetogenic bacteria (homoacetogen medium, 1 g L^{-1} yeast extract) and a marine minimal salt medium (methanogen medium, salinity of 30 g kg^{-1}), cf. Fig. 2b, hydrogen evolution rates by CoP, MoS_2, and NiMo electrodes were not significantly affected, indicating insensitivity of the materials towards the presence of essential growth compounds. In the complex homoacetogen medium, a slightly increased current density (+10%) was observed for both CoP and MoS_2 (see Supplementary Table 1), while the corresponding coulombic efficiencies were slightly reduced from 94.0% and 96.0% to 84.7% and 83.0%, respectively (see Fig. 2b). This reduction in electron recovery was likely due to unspecific reduction reactions of organic compounds (from supplemented yeast extract) on the cathode surfaces, which seems to negatively affect the selectivity for H_2 of both materials under these conditions. In summary, all three cathode materials exhibited relatively high selectivity for HER and remarkably stable performance under biological relevant conditions.

Integrated bioelectrochemical synthesis of methane and acetic acid. Next, we investigated the performance of CoP, MoS_2, and NiMo electrodes in integrated bioelectrochemical systems for microbial production of acetate and methane from CO_2 and electricity. In this proof-of-concept study, 1 cm^2 flat cathodes were introduced into H-type, two-chamber reactors that are used for microbial electrochemistry[45]. A constant current of 1 mA cm^{-2} was applied to the cathodes while CO_2 was provided as 20 vol/vol % in N_2 gas atmosphere in the reactor headspace. These conditions provide an optimal environment for the selected microbial conversions, therefore excluding a limitation of the overall process by the microbial component.

In one set of experiments, the homoacetogenic bacterium *Sporomusa ovata*, which metabolizes CO_2 and H_2 to acetate (Eq. (1)), was introduced as microbial organism to investigate production of acetate as a liquid chemical. In a second set of experiments, we used the methanogenic archaeon *Methanococcus maripaludis* that reduces CO_2 with H_2 to CH_4 (Eq. (2)), to investigate the production of a stable, gaseous hydrocarbon for energy storage.

$$2\,CO_2 + 4\,H_2 \rightarrow CH_3COOH + 2\,H_2O \qquad (1)$$

$$CO_2 + 4\,H_2 \rightarrow CH_4 + 2\,H_2O \qquad (2)$$
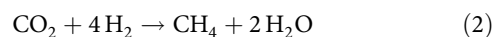
Electrocatalytically produced H_2 was efficiently used by both microorganisms for CO_2 reduction to acetate and methane, respectively, at high selectivity (Fig. 3, Supplementary Fig. 2 and Supplementary Table 2). Electron recovery in the respective product was near 100% in each case (see Supplementary Table 2). Figure 3 shows the production of acetate and methane in the integrated bioelectrochemical system using a NiMo cathode and *S. ovata* and *M. maripaludis*, respectively. The performance of the same system using CoP and MoS_2 is summarized in Supplementary Fig. 2 and Table 2. Importantly, no H_2 gas was detected (<1 vol/vol%) in the reactor headspace of each experiment throughout the entire duration of 48 h, indicating efficient and stable microbial uptake of the electrochemically produced H_2 despite its low solubility in aqueous solutions. In fact, microsensor measurements[46] of H_2 concentration profiles in the bioelectrochemical system revealed elevated H_2 concentrations only in close proximity, 50–100 μm, of the cathode surface (cf. Supplementary Fig. 3d). While the aqueous H_2 concentration in abiotic, Ni–Mo cathode-containing reactors was around 220 μmol L^{-1}, the presence and metabolism of *M. maripaludis* reduced that concentration to 0.2–0.6 μmol L^{-1} (cf. Supplementary Fig. 3a, c). Such efficient transfer of electrons from cathode into the microbial metabolism via hydrogen without the accumulation of high gas concentrations is an important feature of this directly integrated system for two main reasons: first, the use of H_2 as intermediate circumvents the requirement of microbial electrosynthesis for a direct electron transfer and, therefore, extends the spectrum of microbial production hosts to possibly any gas fermenting microorganism. And secondly, the efficient H_2 uptake close to the electrode surface could enable increased production rates as it is known that production rates in gas fermentation are commonly hydrogen limited[15,47]. Future research aiming to balance and maximize rates between inorganic HER and microbial CO_2 reduction will facilitate engineering efforts to further advancing the technology[29].

Notably, the cathode potentials to supply a constant current of 1 mA cm^{-2} for all three materials did not change significantly during the period of 48 h (cf. Fig. 3 and Supplementary Table 2). The maximum change in cathode potential was 193 mV observed for CoP in the setup using *M. maripaludis*, while NiMo showed the highest stability with potential changes as low as 60 mV (cf. Supplementary Table 2). An increase in reduction potential under
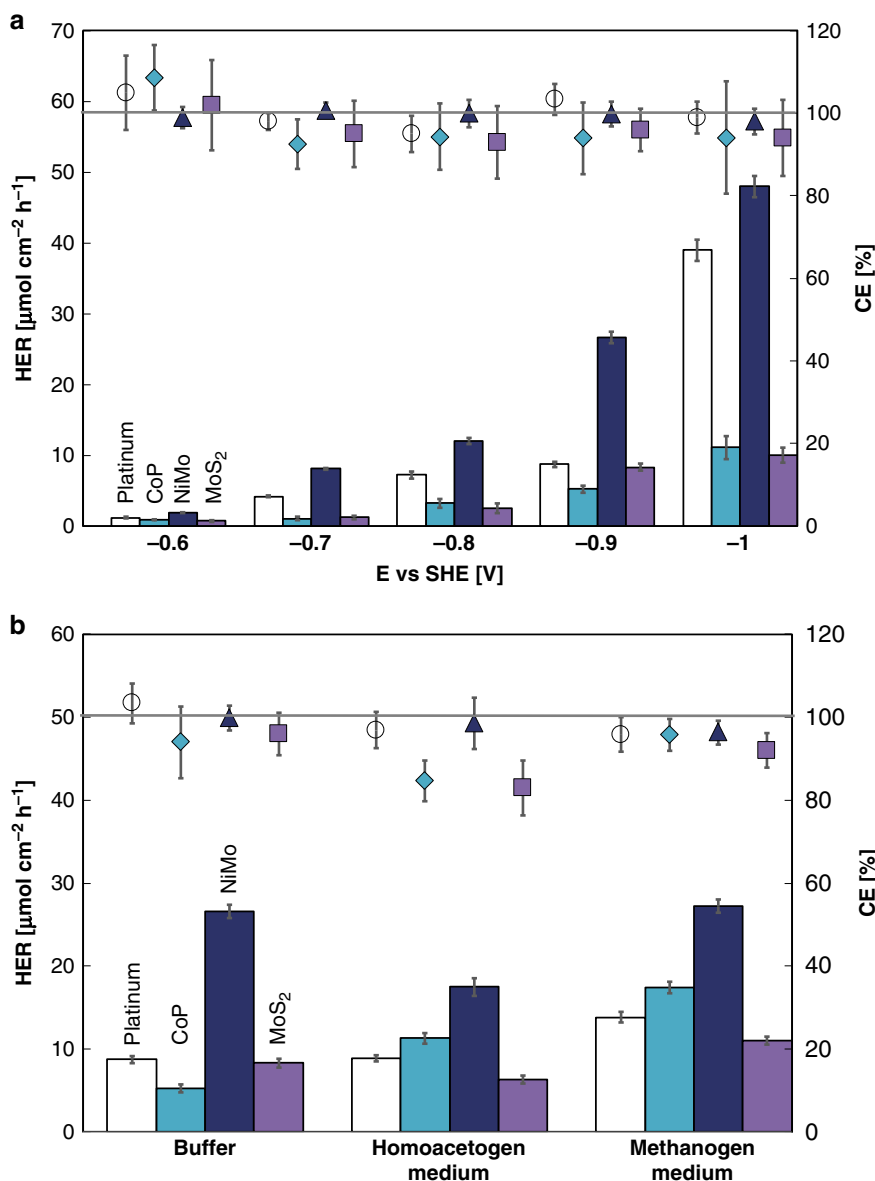
Fig. 2 Hydrogen evolution rates under biocompatible conditions. Hydrogen evolution rates (HER, bar graph, left axis) and corresponding coulombic efficiencies (CE, scatter plot, right axis) of CoP, MoS_2, and NiMo cathodes compared to platinum, the benchmark catalyst for H_2 production. White bars and circles: platinum; turquoise bars and diamonds: CoP; dark blue bars and triangles: NiMo; purple bars and squares: MoS_2. **a** At different potentials in 0.03 M sodium-bicarbonate buffer, pH 7. **b** At constant potential of -0.9 V vs SHE in 0.03 M $NaHCO_3$-buffer and two different microbial growth media. Homoacetogen medium: modified-DSMZ-879; methanogen medium: modified-DSMZ-141. All reported HERs are averaged over a 3-h period. Given values are the mean of biological triplicates with error bars displaying standard deviations. For more details on experimental conditions, refer to the Methods section

constant current conditions could be caused by blocking of active sites on the HER catalyst surface in the biological system. Microscopy studies did not find evidence for attachment of microbial cells to any of the tested, flat-surface cathodes (data not shown). To investigate potential surface contamination introduced through media supplements or microbial activity, XPS survey and high-resolution scans of the electrode materials were performed before and after the operation in the integrated bioelectrochemical system. All three materials showed significant accumulation of various elements after the biotic experiments (cf. Supplementary Table 3). Interestingly, however, HER activity and selectivity were retained despite these accumulations, indicating a good stability of the catalytic activity for HER even in highly supplemented electrolytes. Further, the stable selectivity for H_2 as

single product conferred outright biocompatibility, and no negative effect on the tested bacteria and archaea on growth or metabolism was observed. This identifies the tested materials CoP, MoS_2, and NiMo as promising cathode materials for direct integration in hydrogen-driven bioelectrochemical systems.

Long-term performance. To test for robustness and long-term stability, we operated the integrated reactor system using a NiMo cathode and *M. maripaludis* for 10 days (cf. Fig. 4). When the substrate CO_2 was nearly depleted after 65 h, the reactor head-space was exchanged to remove CH_4 and to re-supply gaseous CO_2 (indicated by vertical dashed lines in Fig. 4); the growth medium was not exchanged, and both catalysts, inorganic NiMo,
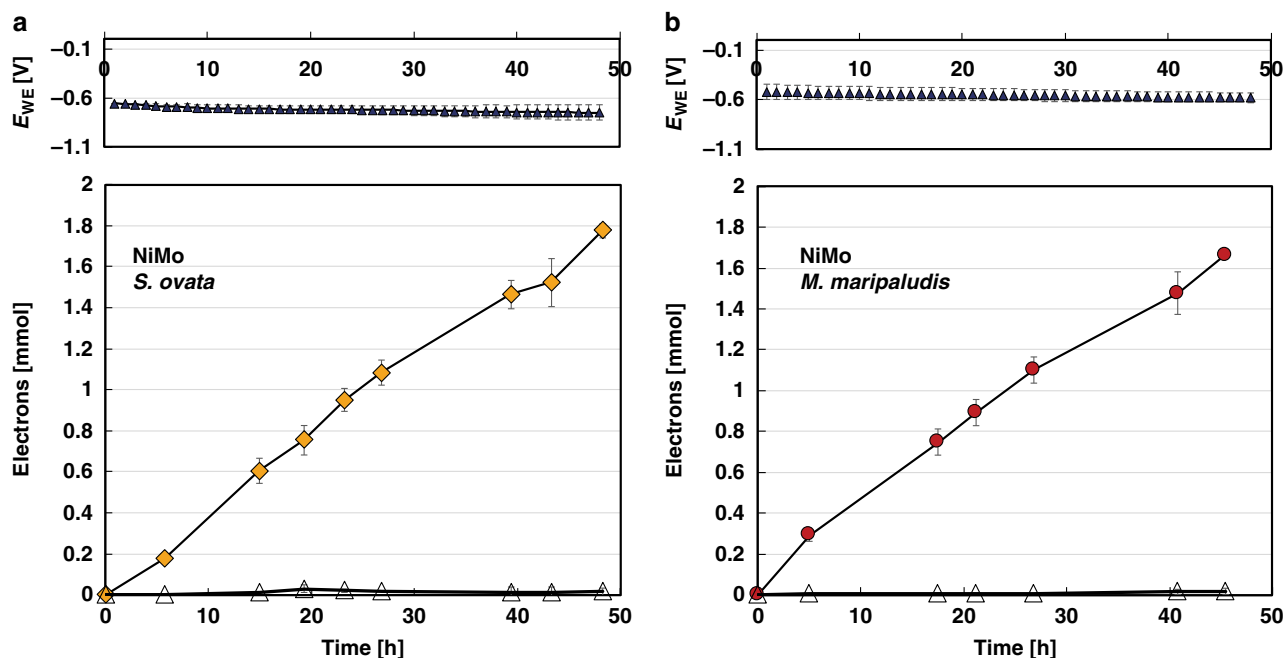
Fig. 3 Bioelectrochemical production of acetate and methane. Performance of integrated bioelectrochemical systems for acetate (**a**) or methane (**b**) formation from CO_2 and electricity, consisting of the two model organisms *Sporomusa ovata* and *Methanococcus maripaludis* and the in situ H_2-producing cathode NiMo. Electrons were supplied with a constant current density of $1\,mA\,cm^{-2}$ and total electrode surface was $1\,cm^2$. The products acetate and methane are plotted as electron equivalents [mmol]. Dotted line: electrons; triangles: hydrogen; yellow diamonds: acetate; red circles: methane; blue triangles in stacked plots: cathode potential vs SHE. Given values are the mean of triplicate experiments with error bars displaying the standard deviation. Electrolyte was microbial growth medium (*S. ovata*: modified-DSMZ-879; *M. maripaludis* modified-DSMZ-141)
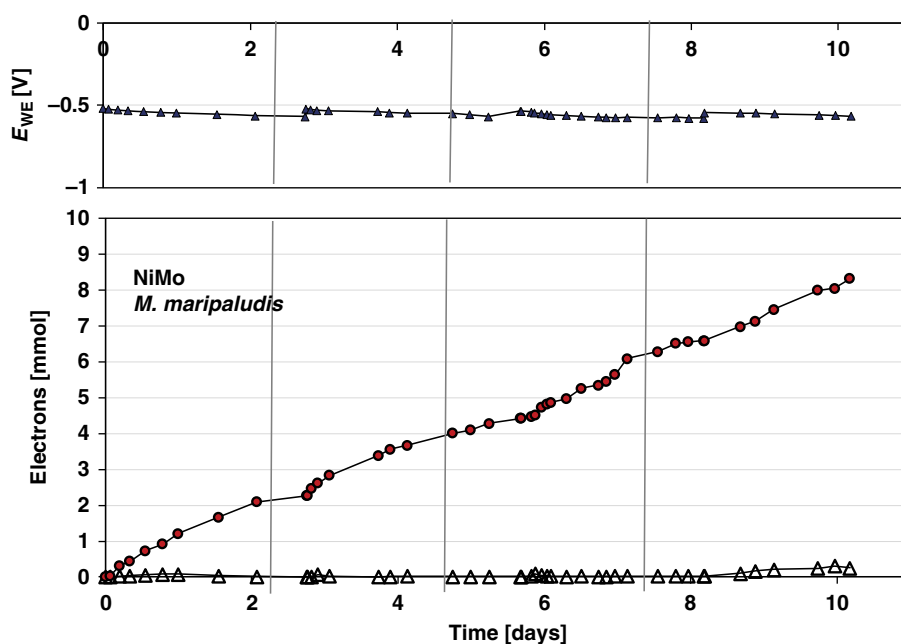

Fig. 4 Long-term performance. Long-term performance of an integrated bioelectrochemical reactor using an NiMo cathode and *Methanococcus maripaludis*. Electrons were supplied as constant current of $1\,mA\,cm^{-2}$ and total electrode surface was 1 mA. The product methane was measured in the gas phase of the reactor and is plotted as electron equivalents. Every 65 h, the reactor headspace was exchanged to remove CH_4 and to re-supply gaseous CO_2 indicated by vertical dashed lines. Dotted line: electrons; hollow triangles: hydrogen; red cycles: methane; solid triangles: cathode potential vs SHE

and biologic *M. maripaludis* remained in the reactor. We continued this operation for a total of four cycles. The results demonstrated a repeatable and stable performance of both catalysts at consistently high coulombic efficiency for methane production from CO_2 utilizing the electrochemically produced

hydrogen for a period of 10 days (see Fig. 4). Coulombic efficiencies were again close to 100% throughout the first three cycles. During the fourth cycle, a slight hydrogen accumulation in the gas phase was noted, which lowered the electron to product recovery to about 95%. This is likely due to a decrease in

microbial activity as medium supplements such as vitamins, trace elements, or reducing agent may have been depleted.

Notably, the HER performance of the NiMo cathode showed very good repeatability over multiple reaction cycles with no evidence of irreversible deactivation. Conventional HER works best at either very high or very low pH, because the concentration of proton donors and/or electrolyte conductivity is maximized[48]. It was shown that at neutral pH, alternative earth-abundant catalysts are able to achieve HER rates comparable to platinum or even outperform platinum-based materials[48–50]. Long-term stability, however, remains a major challenge in these systems. Here, the demonstrated stability over 245 h in highly supplemented electrolyte at neutral pH is therefore particularly promising.

Microbial electrosynthesis beyond known electroactive microbes. In previous studies, only a limited number of microbial species were identified to be able to accept electrons directly derived from a cathode for CO_2 reduction in a process called direct electron transport (DET)[21] while a significant number of microbes were reported to be deficient of DET[18,21]. As the above experiments demonstrated, the use of transition-metal-based cathodes enabled efficient direct integration of microbial electrosynthesis from CO_2 and electricity via in situ produced H_2, thereby circumventing the limiting necessity of a direct microbe–cathode interaction. Therefore, we hypothesized that an H_2-mediated system would enable the cultivation of any microbe capable of metabolic H_2-reduction, including microorganisms categorized as "electro-inactive". To test this hypothesis, we used the homoacetogen *Acetobacterium woodii*, reported to be incapable of DET[21], in our integrated reactor system and observed stable acetate production (see Fig. 5). Similarly to the experiments with *S. ovata* and *M. maripaludis*, hydrogen was taken up and converted into acetate at coulombic efficiency of near 100%. No

toxic effects of the catalyst material towards the microorganism were observed, and, again, the inorganic cathode seemed resistant to biofouling.

Collectively, these results indicate a promising potential for the use of transition-metal-based cathodes for H_2-driven bioelectrochemical systems for production of organic chemicals. The ability to use potentially any autotrophic microorganism in such one-reactor bioelectrochemical system with electricity and CO_2 as the only inputs would significantly expand the microbial platforms and their synthetic capacities for microbial electrosynthesis.

Discussion
Here, we demonstrated a robust and efficient, integrated bioelectrochemical platform for highly selective production of organic compounds from CO_2 using earth-abundant transition-metal-based cathodes. The observed long-term stability of H_2 production on CoP, MoS_2, and NiMo cathodes, despite the accumulation of organic and inorganic material on the electrode surface, demonstrates the potential of this technology to be usable at industrially relevant time scales. Thus, this integrated system provides a robust and scalable pathway to combine electrochemical catalysis and the high selectivity and stability of biological systems. Moreover, the successful integration utilizing the "electro-inactive" *A. woodii* established this system as a platform for many more H_2-utilizing, CO_2-reducing microorganisms. The herein demonstrated production of acetate and methane at high selectivity, rate, and stability can be considered as an entry point for production of a range of industrially relevant chemicals. With the current rapid development of tools for genetic engineering and systems biology, it is expected that both commodity and higher value organic chemicals can be produced in the near future via this platform[15,16,51–53], which is based only on an electron supply via biocompatible cathodes, electricity, CO_2, and microorganisms.
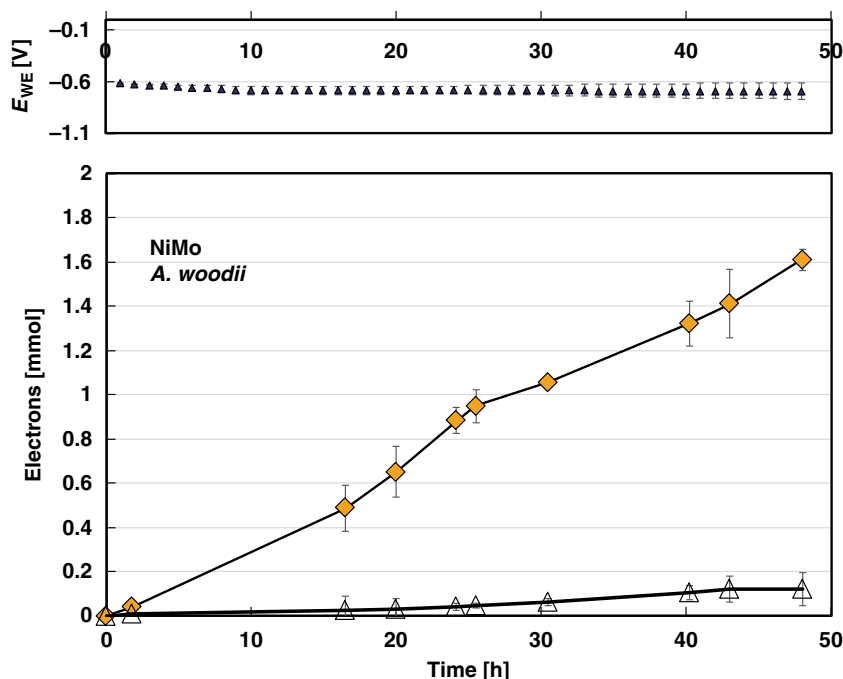

Fig. 5 Electric production by a non-electroactive microbe. Demonstration of acetate production in a directly integrated bioelectrochemical system by the homoacetogen *Acetobacterium woodii*, known to be incapable of DET[21]. Electrons were supplied via a NiMo cathode at constant current density of $1 \, mA \, cm^{-2}$. Electrolyte was microbial growth medium modified-DSMZ-135. The product acetate was measured in the liquid phase of the reactor and is plotted as electron equivalents. Dotted line: electrons; hollow triangles: hydrogen; yellow diamonds: acetate; solid triangles: cathode potential vs SHE. Error bars represent standard deviation between biological triplicates

Methods

Electrode fabrication. Transition-metal-based cathodes were fabricated as flat films on silicon substrates via the following methods. CoP and MoS_2 were prepared as previously described using physical vapor deposition followed by phosphidation or sulfidation, respectively[40,54,55]. For preparation of CoP, ~50 nm of Co was evaporated onto a clean, degenerately doped n-type Si wafer. Subsequently the samples were phosphidized at elevated temperatures in a multi-zone furnace using red phosphorus as a precursor upstream with H_2 gas flowing. For preparation of MoS_2, ~3.6 nm of Mo was sputtered onto a clean degenerately doped p-type Si wafer and subsequently sulfidized at 250 °C for 1 h while flowing an H_2/H_2S gas mixture. Platinum and NiMo layers were prepared directly by physical vapor deposition onto clean, degenerately doped Si wafer substrates. The NiMo was achieved using dual-source, co-evaporation of Ni and Mo. The resulting coatings were of approximate thickness of 100 nm. Based on the film thickness, planar area, and density of the crystal structure we estimate the following specific loadings: Co in CoP: 4.4×10^{-2} mg cm^{-2} Co; Mo in MoS_2: 3.7×10^{-3} mg cm^{-2} Mo; Pt: 2.15×10^{-1} mg cm^{-2} Pt, and NiMo: 9.6×10^{-2} mg cm^{-2} NiMo.

The material was cut into 1 cm^2 pieces and contacted on the backside to a titanium wire, thickness 0.7 mm, with conductive epoxy (Chemtronics CW2400), resulting in an electrical connection with less than 2 Ω resistance. The connection and entire backside was covered with medical grade epoxy (Loctite, EA M-121HP), leaving only the deposited film as active surface. All fabricated electrodes were stored in a desiccator under vacuum for a maximum time of 2 weeks. A photograph of the electrodes is given in Supplementary Figure 1.

Microbial strains and growth conditions. *M. maripaludis* (wild-type strain MM901[56]) was cultured on modified DSMZ medium 141, omitting Na-acetate, yeast extract, trypticase, Na-resazurin, and buffered with 100 mM morpholine-propanesulfonic acid (MOPS) at pH 7. *S. ovata* (wild-type strain DSM 3300) was cultured on modified DSMZ medium 879 omitting fructose and Na-resazurin, and buffered with 100 mM 2-(N-morpholino)ethanesulfonic acid (MES) at pH 5.9. *A. woodii* (wild-type strain DSM 1030) was cultured on modified DSMZ medium 135 omitting fructose and Na-resazurin, and buffered with 100 mM MOPS at pH 7. In both media, modified DSMZ879 and modified DSMZ135, the yeast extract content was reduced to 1 g L^{-1}. Further, in all media Na_2S was omitted (to avoid stripping of gaseous H_2S), while the concentration of L-cysteine was doubled to ensure reduced conditions. Cultures were routinely grown under CO_2/H_2 (20/80% v/v) gas atmosphere. Cultures were inoculated with 2% (v/v) of an exponentially growing culture and grown at 30 °C and 200 r.p.m. For bioelectrochemical experiments, cells were harvested in the late exponential phase at an optical density (OD_{600}) of 0.35–0.45, twice pelleted (5000 r.p.m., 5 min, 30 °C), and resuspended in fresh medium under anaerobic conditions.

For all different microbe species tested in this study and for every media employed here, no growth or production of methane/acetate was observed in the absence of either H_2 or a negatively poised cathode, indicating that a small amount of yeast extract or other media components were not sufficient to support growth and/or product formation.

Integrated bioelectrochemical system. The bioelectrochemical reactors are customized two-chambered borosilicate gastight H-cells (Adams & Chittenden, Scientific Glass, Berkeley, CA, USA). The two chambers have a volume of 150 mL each and were separated by a Nafion 117 proton-exchange membrane (Fuel Cell Store Inc., College Station, TX, USA, surface area 7.5 cm^2). The membrane prevents the transfer of oxygen into the cathode chamber to ensure anaerobic conditions and to prevent the formation of reactive oxygen species at the cathode as reported previously[34]. Each chamber was filled with 100 mL electrolyte under anaerobic conditions (bicarbonate buffer or growth medium, depending on experiment), magnetically stirred at 200 r.p.m., and the gas atmosphere was CO_2/ N_2 (20/80% v/v). In each chamber the electrode was inserted via a gastight rubber stopper from the top of the bottle, while an additional Ag/AgCl reference electrode (NaCl saturated; RE-5B, BASI) was inserted into the cathode chamber via a rubber stopper side port. As anode, a platinized titanium mesh (1″ × 4″, TWL, Amazon.com) was used and the cathode was a 1 cm^2 electrode of the studied cathode materials, fabricated as reported above. Electrochemical experiments were run as constant current or constant potential using a multichannel potentiostat (VMP3; Bio-Logic Science Instruments, Seyssinet-Pariset, France). Before each experiment, the resistance of the setup was determined via electrochemical impedance spectroscopy as standard procedure with subsequent correction of the measured electrode potentials via EC-Lab software (version 11.21, Bio-Logic Science Instruments). All potentials indicated in this article are relative to SHE.

The electrochemical reactors were operated in a temperature-controlled room at 30 °C. Each experiment was started with a fresh, unused cathode. For bioelectrochemical experiments, microbial cultures were added as concentrated, washed cell suspensions to a start OD_{600} of 0.2 inside the cathode chamber. Each experiment was performed as a closed batch system in three independent, biological replicates.

Analytical methods. The gaseous compounds methane and hydrogen were measured using a gas chromatograph (equipped with a thermal conductivity detector and a flame ionization detection detector) as described previously[57]. Acetate and other liquid metabolites were measured via high-performance liquid chromatography equipped with an organic acid column as described previously[57]. To allow comparison of electron uptake rates during the formation of different target products and to visualize electron to product recovery, concentrations of H_2, CH_4, and acetate are given as electron equivalents by multiplying the measured concentrations of the respective compound by the number of electrons required for its formation.

Coulombic efficiencies were calculated by dividing the electrons recovered in products by the electrons supplied as current at a certain time point.

Hydrogen profiles using microsensor measurements. Concentration profiles of H_2 were recorded with commercially available H_2 microsensors (Unisense A/S) and H_2 microsensors with a sulfide frontguard. The H_2 microsensors had a tip size of 20–40 μm and a sensitivity of 0.8–1.2 pA μM^{-1}. The H_2 microsensors were connected to a picoamperemeter, which was connected to an AD-converter connected to a computer. When profiling the microsensors were mounted in a motorized micromanipulator controlled by the software Sensortrace Pro (Unisense A/S) that also recorded the microsensor signals.

Profiling in the bioelectrochemical reactors was achieved by introducing the microsensor through a hole in the rubber stopper lid, which allowed for automated movement of the sensor. To ensure anoxic conditions, the headspace was constantly flushed with anoxic gas: CO_2/N_2 (20/80% v/v). Except for the microsensor insertion and headspace flushing, the reactor setup was identical to the description above. Profiles were recorded from the gas phase down to the cathode surface at 500 μm steps while detailed profiles at the cathode surface were recorded with 50 μm steps. Profiling ceased when a change in the sensor signal indicated that the sensor was touching the cathode surface. In the recorded profiles, the last measurement point unaffected by cathode surface contact was defined as first point within 50 μm of the cathode surface. Recorded profiles are summarized in Supplementary Fig. 3.

Cathode surface characterization. The characterization of surface compositions of the cathodes before and after electrochemical reactions was performed via XPS. The measurements were collected on a Phi Versaprobe III instrument using high-power mode to collect survey scans with charge neutralization enabled after Ar gas-cluster cleaning to partially remove excess organics from the surface. Acquired spectra were quantified using the Multipak software package and presented in a summary format in Supplementary Table 3.

Data availability

The authors declare that all the other data supporting the findings of this study are available within the article and its supplementary information files and from the corresponding author upon request.

References

1. Aresta, M. *Carbon Dioxide as Chemical Feedstock* (John Wiley & Sons, Weinheim, Germany 2010).
2. Harnisch, F., Rosa, L. F., Kracke, F., Virdis, B. & Krömer, J. O. Electrifying white biotechnology: engineering and economic potential of electricity-driven bio-production. *ChemSusChem* **8**, 758–766 (2015).
3. Bushuyev, O. S. et al. What should we make with CO_2 and howow can we make it? *Joule* **2**, 825–832 (2018).
4. Durst, J. et al. Electrochemical CO2 reduction—a critical view on fundamentals, materials and applications. *CHIMIA Int. J. Chem.* **69**, 769–776 (2015).
5. Hori, Y. I. in *Modern Aspects of Electrochemistry* 89–189 (Springer, Berlin, 2008).
6. Ma, S. & Kenis, P. J. Electrochemical conversion of CO_2 to useful chemicals: current status, remaining challenges, and future opportunities. *Curr. Opin. Chem. Eng.* **2**, 191–199 (2013).
7. Kortlever, R., Shen, J., Schouten, K. J. P., Calle-Vallejo, F. & Koper, M. T. Catalysts and reaction pathways for the electrochemical reduction of carbon dioxide. *J. Phys. Chem. Lett.* **6**, 4073–4082 (2015).
8. Möller, T. et al. Efficient CO_2 to CO electrolysis on solid Ni–N–C catalysts at industrial current densities. *Energy Environ. Sci.* **12**, 640–647 (2019).
9. Verma, S., Kim, B., Jhong, H. R. M., Ma, S. & Kenis, P. J. A gross-margin model for defining technoeconomic benchmarks in the electroreduction of CO_2. *ChemSusChem* **9**, 1972–1979 (2016).
10. Weber, R. S. Effective use of renewable electricity for making renewable fuels and chemicals. *ACS Catal.* **9**, 946–950 (2019).

11. Liu, B., Zhang, L., Xiong, W. & Ma, M. Cobalt-nanocrystal-assembled hollow nanoparticles for electrocatalytic hydrogen generation from neutral-pH water. *Angew. Chem. Int. Ed.* **55**, 6725–6729 (2016).

12. Sun, Y. et al. Electrodeposited cobalt-sulfide catalyst for electrochemical and photoelectrochemical hydrogen generation from water. *J. Am. Chem. Soc.* **135**, 17699–17702 (2013).

13. Cobo, S. et al. A Janus cobalt-based catalytic material for electro-splitting of water. *Nat. Mater.* **11**, 802–807 (2012).

14. Xiu, S. et al. Hydrogen-mediated electron transfer in hybrid microbial-inorganic system and application in energy and environment. *Energy Technol.* https://doi.org/10.1002/ente.201800987 (2019).

15. Dürre, P. & Eikmanns, B. J. C1-carbon sources for chemical and fuel production by microbial gas fermentation. *Curr. Opin. Biotechnol.* **35**, 63–72 (2015).

16. Woo, J. E., Song, S. M., Lee, S. Y. & Jang, Y.-S. in *Consequences of Microbial Interactions with Hydrocarbons, Oils, and Lipids: Production of Fuels and Chemicals* (ed. Sang Yup Lee) 1–16 (Springer International Publishing, Cham, Switzerland 2017).

17. Lovley, D. R. & Nevin, K. P. Electrobiocommodities: powering microbial production of fuels and commodity chemicals from carbon dioxide with electricity. *Curr. Opin. Biotechnol.* **24**, 385–390 (2013).

18. Kracke, F., Vassilev, I. & Krömer, J. O. Microbial electron transport and energy conservation—the foundation for optimizing bioelectrochemical systems. *Front. Microbiol.* **6**, 575 (2015).

19. Cheng, S., Xing, D., Call, D. F. & Logan, B. E. Direct biological conversion of electrical current into methane by electromethanogenesis. *Environ. Sci. Technol.* **43**, 3953–3958 (2009).

20. Ganigué, R., Puig, S., Batlle-Vilanova, P., Balaguer, M. D. & Colprim, J. Microbial electrosynthesis of butyrate from carbon dioxide. *Chem. Commun.* **51**, 3235–3238 (2015).

21. Nevin, K. P. et al. Electrosynthesis of organic compounds from carbon dioxide is catalyzed by a diversity of acetogenic microorganisms. *Appl. Environ. Microbiol.* **77**, 2882–2886 (2011).

22. Vassilev, I. et al. Microbial electrosynthesis of isobutyric, butyric, caproic acids and corresponding alcohols from carbon dioxide. *ACS Sustain. Chem. Eng.* **6**, 8485–8493 (2018).

23. Arends, J. B., Patil, S. A., Roume, H. & Rabaey, K. Continuous long-term electricity-driven bioproduction of carboxylates and isopropanol from CO_2 with a mixed microbial community. *J. CO2 Utilization* **20**, 141–149 (2017).

24. Rabaey, K., Girguis, P. & Nielsen, L. K. Metabolic and practical considerations on microbial electrosynthesis. *Curr. Opin. Biotechnol.* **22**, 371–377 (2011).

25. Zeng, M. & Li, Y. Recent advances in heterogeneous electrocatalysts for the hydrogen evolution reaction. *J. Mater. Chem. A* **3**, 14942–14962 (2015).

26. Haas, T., Krause, R., Weber, R., Demler, M. & Schmid, G. Technical photosynthesis involving CO_2 electrolysis and fermentation. *Nat. Catal.* **1**, 32–39 (2018).

27. Ramachandriya, K. D. et al. Carbon dioxide conversion to fuels and chemicals using a hybrid green process. *Appl. Energy* **112**, 289–299 (2013).

28. Torella, J. P. et al. Efficient solar-to-fuels production from a hybrid microbial-water-splitting catalyst system. *Proc. Natl Acad. Sci. USA* **112**, 2337–2342 (2015).

29. Takors, R. et al. Using gas mixtures of CO, CO_2 and H_2 as microbial substrates: the do's and don'ts of successful technology transfer from laboratory to production scale. *Microb. Bbiotechnol.* **11**, 606–625 (2018).

30. Bajracharya, S. et al. Biotransformation of carbon dioxide in bioelectrochemical systems: state of the art and future prospects. *J. Power Sources* **356**, 256–273 (2017).

31. Zhang, T. et al. Improved cathode materials for microbial electrosynthesis. *Energy Environ. Sci.* **6**, 217–224 (2013).

32. Nie, H. et al. Improved cathode for high efficient microbial-catalyzed reduction in microbial electrosynthesis cells. *Phys. Chem. Chem. Phys.* **15**, 14290–14294 (2013).

33. Gimkiewicz, C., Hegner, R., Gutensohn, M. F., Koch, C. & Harnisch, F. Study of electrochemical reduction of CO_2 for future use in secondary microbial electrochemical technologies. *ChemSusChem* **10**, 958–967 (2017).

34. Liu, C., Colón, B. C., Ziesack, M., Silver, P. A. & Nocera, D. G. Water splitting–biosynthetic system with CO2 reduction efficiencies exceeding photosynthesis. *Science* **352**, 1210–1213 (2016).

35. Eftekhari, A. Electrocatalysts for hydrogen evolution reaction. *Int. J. Hydrogen Energy* **42**, 11053–11077 (2017).

36. Yuan, H. & He, Z. Platinum group metal-free catalysts for hydrogen evolution reaction in microbial electrolysis cells. *Chem. Rec.* **17**, 641–652 (2017).

37. Vesborg, P. C. & Jaramillo, T. F. Addressing the terawatt challenge: scalability in the supply of chemical elements for renewable energy. *RSC Adv.* **2**, 7933–7947 (2012).

38. Miao, J. et al. Hierarchical Ni-Mo-S nanosheets on carbon fiber cloth: a flexible electrode for efficient hydrogen generation in neutral electrolyte. *Sci. Adv.* **1**, e1500259 (2015).

39. Strmcnik, D. et al. Improving the hydrogen oxidation reaction rate by promotion of hydroxyl adsorption. *Nat. Chem.* **5**, 300–306 (2013).

40. Landers, A. T. et al. The predominance of hydrogen evolution on transition metal sulfides and phosphides under CO_2 reduction conditions: an experimental and theoretical study. *ACS Energy Lett.* **3**, 1450–1457 (2018).

41. Cave, E. R. et al. Trends in the catalytic activity of hydrogen evolution during CO_2 electroreduction on transition metals. *ACS Catal.* **8**, 3035–3040 (2018).

42. Zhang, Y.-J., Sethuraman, V., Michalsky, R. & Peterson, A. A. Competition between CO_2 reduction and H_2 evolution on transition-metal electrocatalysts. *ACS Catal.* **4**, 3742–3748 (2014).

43. Shinagawa, T. & Takanabe, K. Electrocatalytic hydrogen evolution under densely buffered neutral pH conditions. *J. Phys. Chem. C* **119**, 20453–20458 (2015).

44. Jeremiasse, A. W., Hamelers, H. V., Kleijn, J. M. & Buisman, C. J. Use of biocompatible buffers to reduce the concentration overpotential for hydrogen evolution. *Environ. Sci. Technol.* **43**, 6882–6887 (2009).

45. Deutzmann, J., Sahin, M. & Spormann, A. Extracellular enzymes facilitate electron uptake in biocorrosion and bioelectrosynthesis. *MBio* **6**, e00496–00415 (2015).

46. Nielsen, M., Larsen, L. H., Ottosen, L. D. M. & Revsbech, N. P. Hydrogen microsensors with hydrogen sulfide traps. *Sens. Actuators B Chem.* **215**, 1–8 (2015).

47. Yasin, M. et al. Microbial synthesis gas utilization and ways to resolve kinetic and mass-transfer limitations. *Bioresour. Technol.* **177**, 361–374 (2015).

48. Roger, I., Shipman, M. A. & Symes, M. D. Earth-abundant catalysts for electrochemical and photoelectrochemical water splitting. *Nat. Rev. Chem.* **1**, 0003 (2017).

49. Harnisch, F., Sievers, G. & Schröder, U. Tungsten carbide as electrocatalyst for the hydrogen evolution reaction in pH neutral electrolyte solutions. *Appl. Catal. Environ.* **89**, 455–458 (2009).

50. Callejas, J. F. et al. Electrocatalytic and photocatalytic hydrogen production from acidic and neutral-pH aqueous solutions using iron phosphide nanoparticles. *ACS Nano* **8**, 11101–11107 (2014).

51. Daniell, J., Nagaraju, S., Burton, F., Köpke, M. & Simpson, S. D. in *Anaerobes in Biotechnology* (eds. Hatti-Kaul R., Mamo G. and Mattiasson B. 293–321 (Springer, Berlin, 2016).

52. Marcellin, E. et al. Low carbon fuels and commodity chemicals from waste gases–systematic approach to understand energy metabolism in a model acetogen. *Green Chem.* **18**, 3020–3028 (2016).

53. Schiel-Bengelsdorf, B. & Dürre, P. Pathway engineering and synthetic biology using acetogens. *Febs Lett.* **586**, 2191–2198 (2012).

54. Hellstern, T. R., Benck, J. D., Kibsgaard, J., Hahn, C. & Jaramillo, T. F. Engineering cobalt phosphide (CoP) thin film catalysts for enhanced hydrogen evolution activity on silicon photocathodes. *Adv. Energy Mater.* **6**, 1501758 (2016).

55. Benck, J. D. et al. Designing active and stable silicon photocathodes for solar hydrogen production using molybdenum sulfide nanomaterials. *Adv. Energy Mater.* **4**, 1400739 (2014).

56. Costa, K. C. et al. Protein complexing in a methanogen suggests electron bifurcation and electron delivery from formate to heterodisulfide reductase. *Proc. Natl. Acad. Sci. USA* **107**, 11050–11055 (2010).

57. Lohner, S. T., Deutzmann, J. S., Logan, B. E., Leigh, J. & Spormann, A. M. Hydrogenase-independent uptake and metabolism of electrons by the archaeon Methanococcus maripaludis. *ISME J.* **8**, 1673–1681 (2014).

Author contribution

F.K. fabricated the electrodes, designed, and performed the experiments in the abiotic as well as integrated bio-electrochemical system, analyzed the data, and drafted the manuscript. A.B.W. performed physical vapor deposition for electrode synthesis and performed and analyzed all XPS measurements. K.M. performed the microsensor measurements and analyzed the data. M.A.H. assisted in electrode fabrication. F.K., A.B.W., J.S.D., C.H., T.F.H. and A.M.S. conceived and designed the study and contributed in

regular data analyzes and discussions. All authors edited, read, and approved the final manuscript.

Additional information

Supplementary information accompanies this paper at https://doi.org/10.1038/s42004-019-0145-0.

Competing interests: The authors declare no competing interests.

Reprints and permission information is available online at http://npg.nature.com/reprintsandpermissions/

Publisher's note: Springer Nature remains neutral with regard to jurisdictional claims in published maps and institutional affiliations.